DOI: 10.1002/ejic.200901244

1D Chains Constructed from Oxido-Centered [Mn_3O] Units Exhibiting Single-Chain Magnet Behavior

Xueyan Song,[a] PeiPei Yang,[a] Xuelan Mei,[a] Licun Li,*[a] and Daizheng Liao[a]

Keywords: Magnetic properties / Manganese / Chain structures / Structure elucidation

The synthesis, crystal structure, and magnetic properties of two new Mn^{III} single-chain magnets, $[Mn_3O(L)_3(HCOO)(CH_3OH)_4]\cdot 2CH_3OH$ (**1**) and $[Mn_3O(L)_3N_3(C_2H_5OH)_3(H_2O)]$ (**2**) (H_2L = 3-*tert*-butyl-5-methylsalicylaldoxime) are reported. Complexes **1** and **2** consist of a triangle of Mn^{III} ions with an oxido-center bridge and three 3-*tert*-butyl-5-methylsalicylaldoxime ligands that form a plane with the metal ions. Both complexes contain the same cores with the general formula $[Mn_3(\mu_3\text{-}O)(L)_3]^+$, which are further connected by formate (complex **1**) or azide (complex **2**) ligands into chain structures. Temperature-dependent magnetic susceptibility studies indicate the presence of antiferromagnetic interactions between the Mn^{III} ions in **1**, whereas predominantly ferromagnetic interactions are observed in **2**. Both complexes show slow relaxation of their magnetizations associated with single-chain magnet behavior.

Introduction

Nowadays, the subject of single-molecule magnets (SMMs) and single-chain magnets (SCMs) has become a hot topic of research at the frontier between chemistry and physics because of their unique and intriguing properties and potential applications in high-density data storage technologies and molecular spintronics.[1–5] The former are isolated as zero-dimensional nanoparticles, which exhibit slow relaxation of their magnetization arising from the combination of a large ground-state spin *S* and a high negative *D* value. The first SMM (a Mn_{12} cluster) was discovered by Gatteschi and co-workers in 1993.[6] Since then, several types of SMMs have been reported, and the field is rapidly expanding.[7–14] The latter are nanowires (SCMs), and they possess significant uniaxial anisotropy, and the interchain interactions must be as small as possible (in comparison to the intrachain ones).[15] The first example of a SCM was a Co^{II} polymer bridged by nitronyl nitroxides, reported by Gatteschi and co-workers in 2001.[16] In contrast to the rapid development of SMMs, SCMs are significantly restricted, which may be attributable to the difficulty in arranging these magnetic nanowires while maintaining a sufficiently large ratio of intra- to interchain magnetic interaction to "freeze in" one-dimensional (1D) magnetization and prevent 2D and 3D ordering.[17]

So far, SCMs mainly include 3d–radical,[16,18] 3d–3d,[19] 3d–5d,[20] 3d–4f,[21] and 4f–radical[22] heterospin systems containing at least two different spin carriers. Compared to heterospin SCMs, far fewer homospin SCMs have been reported. The first example of a homospin SCM was an azido-bridged Co^{II} complex in 2003,[23] then pure Mn^{III} systems[24] and a 4f[25] homospin SCM were reported. On the other hand, most of the reported SCMs are ferromagnetic or ferrimagnetic chains. The first example of an unusual type of SCM with antiferromagnetic exchange was reported in 2005[26] concerning the Co^{II} diphosphonate material, and since then SCM properties were also observed in non-colinear antiferromagnetic structures of only a few Mn^{III} and Ni^{II} chain complexes.[24b,27,24a] To gain insight into the fundamental magnetic nature of these systems, more examples are highly sought and different bridging units need to be explored.

Recently, salicylaldoxime derivatives[24b] or pyrazole derivatives[24c,27b,28] have been widely used for the synthesis of low-dimensional magnets, and some oxido-centered Mn^{III} cluster units [Mn^{III}_3 (μ_3-O^{2-})] have been synthesized, which display a diversity of magnetic properties. For example, Tao et al.[27b] reported a novel SCM, $[Mn^{III}_3O(Meppz)_3(EtOH)_4(OAc)]$ [Meppz = 3-(5-methyl-2-phenolate)pyrazolate], which demonstrated the coexistence of magnetization relaxation and dielectric relaxation; Gao et al.[24b] adopted the 3,5-di-*tert*-butylsalicylaldoxime coligand to synthesize two SCMs based on the [$Mn^{III}_3(\mu_3\text{-}O^{2-})$] unit; Reedijk et al.[29] synthesized three new trinuclear μ_3-oxide-bridged Mn^{III} complexes containing 3(5)-(2-hydroxyphenyl)-5(3)-methylpyrazole and 3(5)-(2-hydroxyphenyl)-5(3)-phenylpyrazole; Liu et al.[24c] reported three 1D coordination polymers based on the *anti–anti* carboxylato bridged [$Mn^{III}_3(\mu_3\text{-}O^{2-})$] unit and the Brppz [3-(5-bromine-2-phenolate)pyrazolate] coligand, Solvents have a great influence on the chain structures of these complexes, and quite different magnetic behaviors are observed at low temperatures. Herein, we utilized a new salicylaldoxime derivative 3-*tert*-butyl-5-methylsalicylaldoxime as the coligand of the [$Mn^{III}_3(\mu_3\text{-}O^{2-})$] unit,

[a] Department of Chemistry, Nankai University, Tianjin 300071, P. R. China
E-mail: llicun@nankai.edu.cn

formate, and end-to-end (EE)-azido as the bridge ligands to yield two 1D chainlike complexes, $[Mn_3O(L)_3(HCOO)(CH_3OH)_4]\cdot 2CH_3OH$ (**1**) and $[Mn_3O(L)_3N_3(C_2H_5OH)_3(H_2O)]$ (**2**). DC magnetic studies indicate the presence of antiferromagnetic interactions between the Mn^{III} ions in **1**, and this is a new example of an antiferromagnetic exchange SCM; in complex **2**, unusual ferromagnetic interactions are observed when the trinuclear units are linked by end-to-end azido bridges. Both complexes show clear slow magnetic relaxation behaviors at low temperature.

Results and Discussion

Description of the Molecular Structures

X-ray structural analysis reveals that **1** is composed of single *anti–anti*-formate-bridged $[Mn^{III}_3O(L)_3(MeOH)_4]^+$ triangular cluster units (Figure 1). Selected bond parameters are listed in Table 1. Each $[Mn_3O]$ unit in the chain has two different Mn^{III} ions coordinated by formato bridging ligands. In the $[Mn_3O]$ unit, three Mn^{III} ions are bridged by a central oxygen atom, and the μ_3-O^{2-} (O1) is located 0.041 Å above the Mn_3 plane with Mn–O_{center} bonds of 1.880–1.883 Å; the Mn–O1–Mn angles are 119.46, 120.08, and 120.32° for Mn2–O1–Mn3, Mn1–O1–Mn3, and Mn1–O1–Mn2, respectively. Each edge of the Mn_3 triangle is bridged by the μ_2:η^1:η^1:η^1 L coligand, whose deprotonated hydroxy group is bound terminally to a Mn^{III} ion. All Mn are hexacoordinate with a similar basal plane $[N_1O_3]$ composed of the central μ_3-O^{2-} ion, one N atom and one O atom from one L coligand, and one O atom from another L coligand. Each Mn1 contains two methanol molecules at the axial positions, with a Mn–O_{apical} average distance of 2.271 Å. Mn2 and Mn3 are axially coordinated to a methanol molecule and a formate anion with a Mn–O_{apical} average distance of 2.275 and 2.270 Å, respectively, which is longer than the Mn–$O_{equatorial}$ and Mn–$N_{equatorial}$ bond lengths [1.859–1.950 and 2.001–2.006 Å, respectively]. This means that all Mn^{III} ions display a classical Jahn–Teller (JT) elongation, as expected for the high-spin $3d^4$ Mn^{III} ion. The intracluster Mn···Mn distances are 3.249–3.266 Å.

Each $[Mn_3O]$ unit is connected with adjacent ones by using the formate groups as bridges in the *anti–anti* coordination mode, forming a 1D stepwise chain structure along the *c* axis. The formate-bridged Mn···Mn distance is 6.296 Å, which is a little shorter than that of $[Mn_3O(t\text{Bu-sao})_3(HCOO)(CH_3OH)_4]\cdot CH_3OH\cdot 0.5H_2O$ (6.471 Å),[24b] and the dihedral angle between the adjacent $[Mn_3O]$ planes is 40.8°, probably arising from the bent coordination character of the *anti–anti* formate bridges and the stacking of the alkyl groups between the chains. The shortest interchain Mn···Mn distance is 11.1 Å, which suggests that the chains are well isolated from each other by the bulk alkyl groups of the ligands. Figure 2 displays a packing diagram of complex **1**: there are no hydrogen bonds and no π–π interactions between the chains.

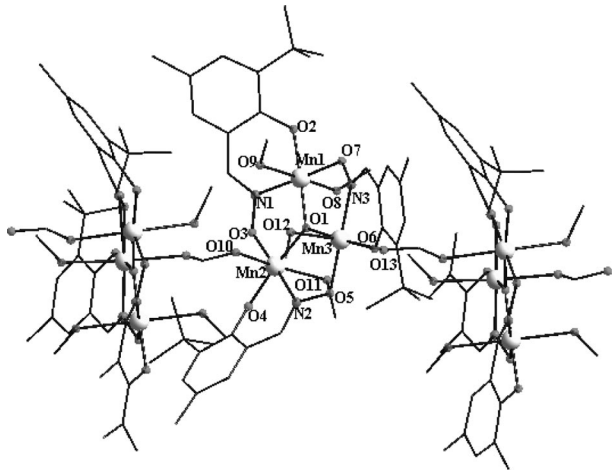

Figure 1. The chain of $[Mn_3O]$ units bridged by formate ions in complex **1**.

Table 1. Selected bond lengths [Å] and angles [°] for complexes **1** and **2**.

Complex **1**		Complex **2**	
Mn1–O2	1.882(3)	Mn1–O7	1.873(2)
Mn1–O1	1.883(3)	Mn1–O1	1.850(3)
Mn1–N1	2.001(5)	Mn1–N1	1.987(3)
Mn1–O8	2.274(4)	Mn1–O8	2.245(3)
Mn2–N2	2.006(4)	Mn2–N2	1.974(3)
Mn2–O1	1.882(4)	Mn2–O7	1.875(2)
Mn3–O1	1.880(3)	Mn3–O7	1.880(2)
Mn3–O10	2.242(4)	Mn3–O11	2.391(3)
O2–Mn1–O1	176.29(16)	O1–Mn1–O7	175.43(14)
O2–Mn1–N1	93.83(8)	O1–Mn1–N1	89.67(13)
O2–Mn1–O9	89.86(15)	O7–Mn1–O8	88.84(11)
O4–Mn2–O1	174.37(16)	O4–Mn2–O1	89.65(13)
O1–Mn2–N2	89.55(16)	O7–Mn2–N2	87.48(11)
O6–Mn3–O1	177.56(15)	O5–Mn3–O7	174.08(11)
O6–Mn3–N3	89.38(16)	O7–Mn3–N3	87.81(11)
Mn1–O1–Mn2	120.32	Mn1–O7–Mn2	121.13
Mn1–O1–Mn3	120.08	Mn1–O7–Mn3	119.55
Mn2–O1–Mn3	119.46	Mn2–O7–Mn3	119.32

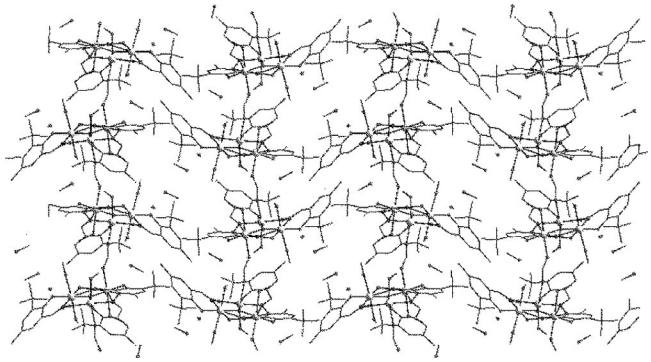

Figure 2. A packing diagram of **1** viewed down the *a* axis.

Replacement of the apical formate by azide gives another chain-like complex $[Mn_3O(L)_3N_3(C_2H_5OH)_3(H_2O)]$ (**2**; Figure 3). Complex **2** has a structure similar to that of **1**. In complex **2**, the $[Mn_3O]$ unit is almost coplanar, the μ_3-O^{2-} (O7) ion lies 0.002 Å above the Mn_3 triangle. Like **1**, there

are three crystallographically independent manganese atoms in **2**. Each Mn atom adopts a distorted octahedral geometry, with a similar basal plane [N_1O_3] to that of **1**. However, in **2**, Mn1 contains two ethanol molecules (O8, O9) at the axial positions, Mn2 contains one water molecule (O10) and one azide molecule (N4) at the axial positions, whereas in Mn3, one ethanol molecule (O11) and one azide molecule (N6) occupy the axial positions. The Mn–O_{apical} distances and Mn–N_{apical} distances [2.239–2.390 and 2.25–2.336 Å, respectively] are obviously longer than the Mn–$O_{equatorial}$ distances and Mn–$N_{equatorial}$ distances [1.847–1.910 and 1.974–1.990 Å, respectively]. The JT axes of all three Mn^{3+} ions in **2** are almost parallel to each other and are approximately perpendicular to the Mn^{III}_3O plane. Selected bond lengths and angles are listed in Table 1. The Mn···Mn distances in the trinuclear unit are 3.264, 3.243, and 3.241 Å for Mn1···Mn2, Mn1···Mn3, and Mn2···Mn3, respectively. The Mn–O7–Mn angles are Mn1–O7–Mn2 121.13°, Mn1–O7–Mn3 119.55°, and Mn2–O7–Mn3 119.32°. The shortest Mn···Mn distance between the trinuclear units is 6.205 Å through the azide bridges, which is slightly shorter than the formate-bridged distance in **1** (6.296 Å) and longer than those in [$Mn_3O(t$Bu-sao$)_3N_3$-$(CH_3OH)_4$]·0.5CH_3OH (5.964 Å).[24b] The shortest interchain Mn···Mn distance is 10.3 Å. In **2**, the adjacent [Mn_3O] planes are parallel to each other (dihedral angle 0°). This feature should be a result of the linear coordination orientation of the EE azide, which is different to the bent one of *anti–anti* formate. The packing diagram of **2** is shown in Figure 4.

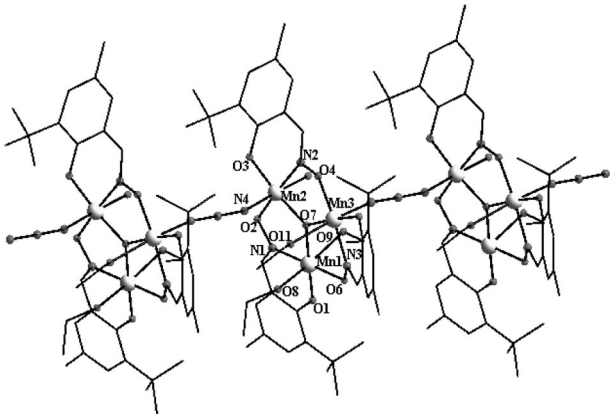

Figure 3. The chain of [Mn_3O] units bridged by azide ions in complex **2**.

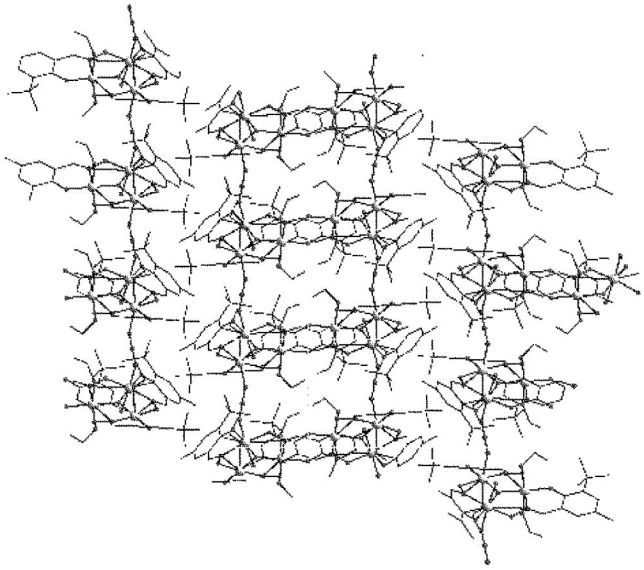

Figure 4. View of the packing arrangement of **2** down the *a* axis.

Magnetic Properties

The magnetic susceptibilities of complexes **1** and **2** were measured in the range 2–300 K in an external magnetic field of 2000 Oe. The plots of $\chi_M T$ for complexes **1** and **2** are shown in Figures 5 and 6, respectively. For **1**, at room temperature, the experimental $\chi_M T$ value is 8.61 $cm^3\,K\,mol^{-1}$, which is somewhat smaller than that expected for three magnetically isolated Mn^{III} ions (9.0 $cm^3\,K\,mol^{-1}$ for g = 2.0). When lowering the temperature, the $\chi_M T$ product decreases gradually to 3.17 $cm^3\,K\,mol^{-1}$ at 2 K. The observed behavior suggests the presence of intramolecular antiferromagnetic interactions between the Mn^{III} ions in the trinuclear units. The data above 9 K were well fitted to the Curie–Weiss law, with C = 10.23 $cm^3\,K\,mol^{-1}$ and θ = –31.4 K. First, we were only concerned with the coupling of the [Mn_3O] unit. On the basis of the crystal structure, a 2J model was used for quantitative analysis of the exchange interactions.[28d] Thus, the susceptibility data were fitted with the Hamiltonian for an isosceles triangle [Equation (1)].

$$\hat{H} = -2J_1\hat{S}_1\hat{S}_2 - 2J_1\hat{S}_1\hat{S}_3 - 2J_2\hat{S}_2\hat{S}_3 \quad (1)$$

where J_1 represents the Mn^{III}–Mn^{III} exchange interaction parameter of the two exchange paths with similar Mn···Mn distances and Mn–O_{oxide}–Mn angles and J_2 refers to the path characterized by the unique Mn–O_{oxide}–Mn angle (Mn2–O1–Mn3). Considering the weak interactions mediated by formate, the susceptibility can be corrected by the mean-field, zJ' with the magnetic susceptibility expression

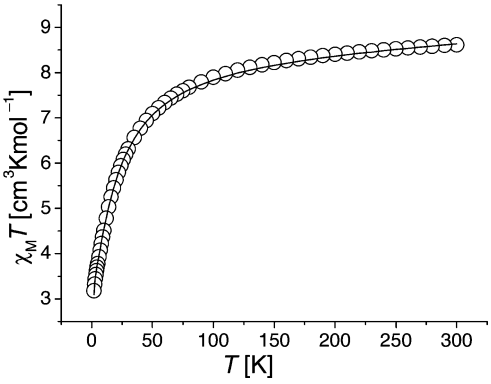

Figure 5. Temperature dependence of the $\chi_M T$ product of **1**. The solid lines are the best-fitted simulation curves based on a 2J model with the mean field zJ' described in the text.

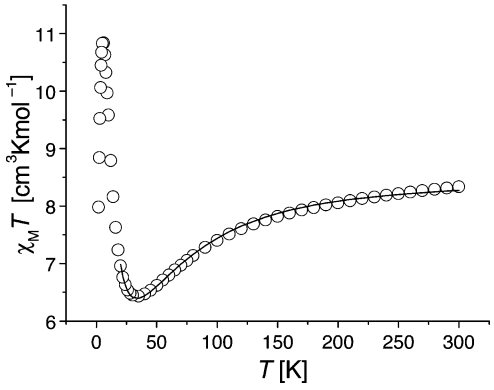

Figure 6. Temperature dependence of the $\chi_M T$ product of **2**. The solid lines are the best-fitted simulation curves based on a 1D chain model described in the text.

$$\chi_M = \frac{\chi_{trimer}}{[1 - \chi_{trimer}(2zj'/Ng^2\beta^2)]}$$

The best parameters fitted in the whole temperature range are $g = 2.06$, $J_1 = -2.79$ cm^{-1}, $J_2 = -1.29$ cm^{-1}, $zJ' = -0.19$ cm^{-1}with $R = 5.6 \times 10^{-4}$ {R value is defined as $\Sigma[(\chi_M)_{obsd.} - (\chi_M)_{calcd.}]^2/\Sigma[(\chi_M)_{obsd.}]^2$}. The negative zJ' value indicates weak antiferromagnetic interactions through the *anti–anti* formato bridges. For **2**, at room temperature, the experimental $\chi_M T$ value is 8.33 cm^3 K mol^{-1}, which is slightly smaller than that expected for three magnetically isolated Mn^{III} ions (9.0 cm^3 K mol^{-1} for $g = 2.0$). Cooling the temperature, the $\chi_M T$ product decreases gradually to 6.47 cm^3 K mol^{-1} at 35 K then increases to a maximum at 6 K, with a value of 10.84 cm^3 K mol^{-1}, and then falls, which may arise from zero-field splitting and/or weak interchain interactions. Compared to the formate bridge, azide is a stronger magnetic coupler. First, similar to **1**, we only concern the coupling of the [Mn_3O] unit and the same magnetic model was used as **1**, J_2 is the Mn1–Mn2 interaction with angle Mn1–O_{oxide}–Mn2 121.13°. Then the best parameters fitted above 20 K are $g = 1.99$, $J_1 = -2.15$ cm^{-1}, $J_2 = -5.57$ cm^{-1}, $zJ' = 1.91$ cm^{-1} with $R = 2.1 \times 10^{-4}$ {R value is defined as $\Sigma[(\chi_M)_{obsd.} - (\chi_M)_{calcd.}]^2/\Sigma[(\chi_M)_{obsd.}]^2$}. However, it should be noted that the value of zJ' is somewhat unreasonable, so we treated the [Mn_3O] cluster as the repeat unit and used a 1D chain model with the Hamiltonian $\hat{H} = -J\Sigma\hat{S}_{T_i}\hat{S}_{T_{i+1}}$ to quantitatively analyze the magnetic data (Scheme 1). The expression of magnetic susceptibility is described by Equation (2).

$$\chi_{chain} = \frac{Ng^2\beta^2}{3kT}[S_T(S_T+1)]\frac{1+u}{1-u}$$
$$u = \coth[J_3 S_T(S_T+1)/kT] - kT/[J_3 S_T(S_T+1)]$$
$$S_T(S_T+1) = 3k\chi_{trimer}T/Ng^2\beta^2 \quad (2)$$

The best parameters fitted above 20 K are $g = 1.99$, $J_1 = -3.08$ cm^{-1}, $J_2 = -6.53$ cm^{-1}, $J_3 = 3.42$ cm^{-1} with $R = 3.1 \times 10^{-5}$. J_3 is the intrachain coupling parameter, $J_3 > 0$ represent ferromagnetic interactions through end-to-end azide bridges.[24b,28b]

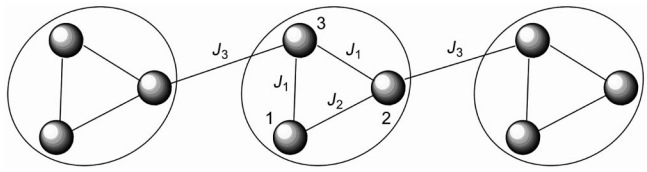

Scheme 1. 1D chain model used for complex **2**.

According to previous theoretical and experimental studies for oxide-centered trinuclear Mn^{III} complexes where the superexchange interaction can change from antiferromagnetic to ferromagnetic when the metal-ion–ligand–metal-ion angle decreases with a critical angle value of around 120°.[29,30] For complexes **1** and **2**, the Mn–O_{oxide}–Mn angles are nearly 120°, and as a consequence, all intracluster magnetic interactions are antiferromagnetic. Similar behavior has also been reported previously in related compounds.[27b,28a,28b] When the trinuclear units are linked by formate bridges, antiferromagnetic interactions emerge between the trinuclear units within the chain, whereas ferromagnetic interactions are observed when the trinuclear units are linked by end-to-end azido bridges.

To probe the magnetization dynamics of **1**, alternating current (ac) susceptibility studies were performed in the 2–15 K range by using a 3.5 G field oscillating at frequencies in the 100–1300 Hz range. The obtained data (Figure 7) reveal that below 5.0 K both the in-phase (χ_M') and out-of-phase (χ_M'') ac susceptibilities are frequency dependent. These data indicate a significant barrier to magnetization relaxation and preclude 3D ordering. The shift of peak temperature (T_f) of χ_M' is measured by a parameter $\phi = (\Delta T_f/T_f)/\Delta(\log f) = 0.15$, which is in the range of normal superparamagnets[19c,24e,31] and excludes the possibility of a spin glass ($0.01 < \phi < 0.1$).[32–35] The magnetization relaxation times obtained from ac experiments were fitted to the Arrhenius equation [Equation (3)].

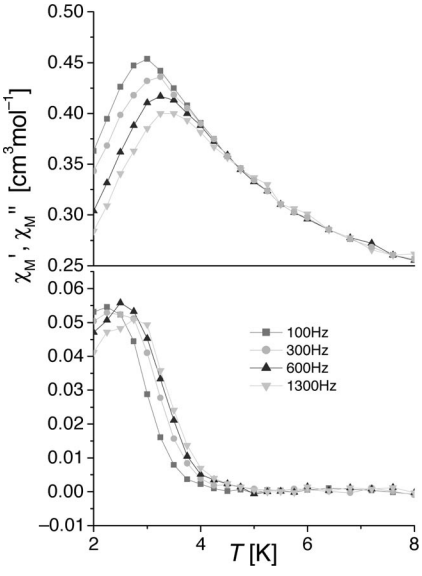

Figure 7. Real χ_M' and imaginary χ_M'' ac magnetic susceptibility of complex **1** in zero dc field with an ac field of 3.5 Oe.

$$\tau_{(T)} = \tau_0 \exp(\Delta_{eff}/k_B T) \quad (3)$$

where Δ_{eff} is the average energy barrier for the reversal of the magnetization, τ_0 is the attempt time, and k_B is the Boltzmann constant. Plots of $1/T_B$ vs. $\ln\tau$ for complex **1** (Figure 8) follow a linear variation that confirms the theoretical predictions of Equation 3. The values of the energy barrier Δ_{eff}/k_B = 51.35 K and $\tau_0 = 5.88 \times 10^{-12}$ s. The dynamics of the magnetization relaxation of **1** suggest classical SCM behavior.

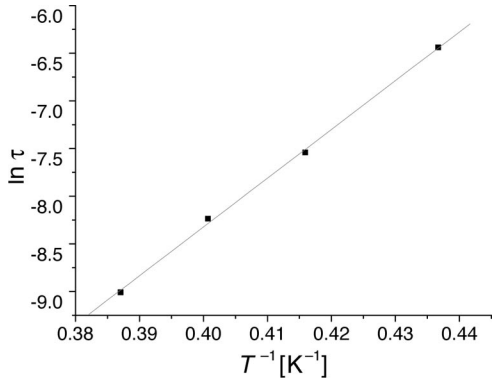

Figure 8. Plots of $\ln\tau$ vs. $1/T_B$ for complex **1**. The solid line represents the least-squares fit of the experimental data to the Arrhenius law.

Alternating current susceptibility studies of complex **2** were performed in the 2–13 K range by using a 3.5 G field oscillating at frequencies in the 50–1300 Hz range. The obtained data (Figure 9) reveal that below 6.0 K both the in-phase (χ_M') and out-of-phase (χ_M'') ac susceptibilities are strongly frequency dependent. Using mentioned equation, $\phi = 0.14$ excludes the possibility of a spin glass; the values of the energy barrier for complex **2** are Δ_{eff}/k_B = 81.92 K

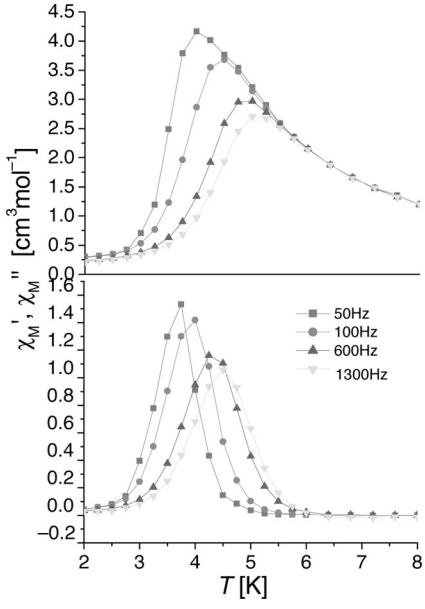

Figure 9. Real χ_M' and imaginary χ_M'' ac magnetic susceptibility of complex **2** in zero dc field with an ac field of 3.5 Oe.

and $\tau_0 = 1.54 \times 10^{-12}$ s. The plot of $1/T_B$ vs. $\ln\tau$ is shown in Figure 10. The field-dependent magnetization at 2 K displays a small butterfly-shaped hysteresis with a coercive field about 150 Oe (Figure 11). A plot of $\ln(\chi_M T)$ against T^{-1} decreases almost linearly[24b,36,37]between 24 and 12 K with an energy gap Δ_ξ/k_B of 7.06 K, thus confirming the 1D nature of **2** (Figure 12). The dynamics of the magnetization relaxation of **2** suggest classical SCM behavior too.

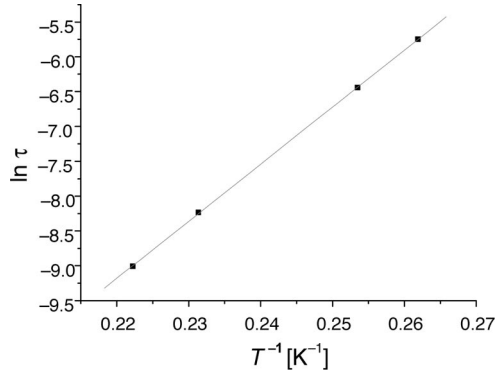

Figure 10. Plots of $\ln\tau$ vs. $1/T_B$ for complex **2**. The solid line represents the least-squares fit of the experimental data to the Arrhenius law.

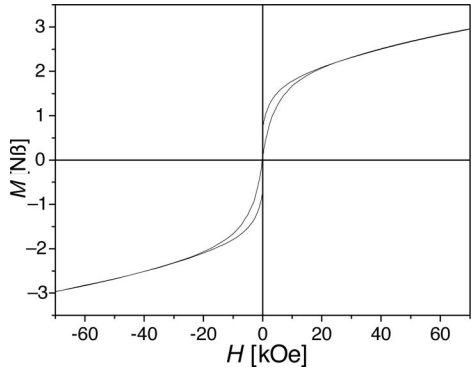

Figure 11. Magnetization (M) vs. applied magnetic field (H) hysteresis loops of complex **2**.

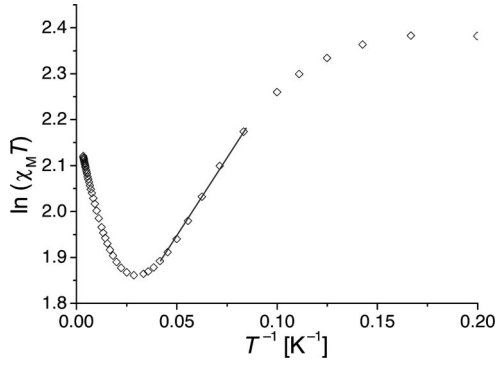

Figure 12. Plot of $\ln(\chi_M T)$ vs. T^{-1} for complex **2**. Solid-line represents the fit to the expression of $\chi T/C = \exp(\Delta_\xi/k_B T)$.

Comparison of the magnetic coupling in compounds **1** and **2** shows that the two kinds of bridges not only mediate the different interactions but also influence the intra-trinu-

clear coupling. We also compare another reported $[Mn_3O]$ cluster[24b] with 3,5-di-*tert*-butylsalicylaldoxime coligand. It appears that the small change of aromatic group substituted or coordinated solvent molecules may greatly influence the magnetic properties. This still needs to be supported by new experimental and theoretical work. So, we recently synthesized another 3,5-dimethylsalicylaldoxime ligand to obtain some new complexes with the hope to further explain the magnetostructural correlations.

Conclusions

The use of the 3-*tert*-butyl-5-methylsalicylaldoxime ligand and formate or azide as bridges gives two new homospin SCMs. Both complexes present overall intramolecular antiferromagnetic interactions between the three Mn^{III} ions comprising the trinuclear unit. In addition, complex **1** is a rare example of antiferromagnetic SCM bridged by formate, whereas complex **2** is another novel example of end-to-end azide bridged ferromagnetic SCM.

Table 2. Crystal data and structure refinements for **1** and **2**.

	1	**2**
Empirical formula	$C_{43}H_{70}Mn_3N_3O_{15}$	$C_{42}H_{65}Mn_3N_6O_{11}$
Molecular mass	1033.84	994.81
T [K]	113(2)	113(2)
Crystal system	monoclinic	monoclinic
Space group	$P2_1/n$	$P2_1/c$
β [°]	91.89(3)	97.78(3)
a [Å]	13.624(3)	18.510(4)
b [Å]	14.388(3)	7.6596(15)
c [Å]	27.041(5)	34.645(7)
V [Å^3]	5450.1(19)	2736.3(9)
Z	4	4
$D_{calcd.}$ [g cm^{-3}]	1.260	1.356
Crystal size	$0.20\times0.16\times0.12$	$0.20\times0.18\times0.14$
μ [mm^{-1}]	0.745	0.827
Unique reflns/R_{int}	9610/0.0643	8494/0.0337
Number of parameters	613	569
GOF	1.096	1.082
R_1[a] [$I>2\sigma(I)$]	0.0740	0.0567
wR_2[b] (all data)	0.2246	0.1597

[a] $R_1 = \Sigma(||F_o| - |F_c||)/\Sigma|F_o|$. [b] $wR_2 = \{\Sigma w(|F_o|^2 - |F_c|^2)^2/\Sigma w|F_o|^2)^2\}^{1/2}$.

Experimental Section

General Remarks: Commercially available reagents were used as received without further purification. The ligands 3-*tert*-butyl-5-methylsalicylalde and 3-*tert*-butyl-5-methylsalicylaldoxime (H_2L) were prepared according to reported procedures.[38,39]

Physical Measurements: Elemental analyses for C, H, and N were performed with a Perkin–Elmer 240 analyzer at the Institute of Elemental Organic Chemistry, Nankai University. IR spectra using KBr pellets were recorded with a Bruker Tensor 27 FTIR spectrophotometer. Variable-temperature magnetic susceptibilities were measured with a SQUID MPMS XL-7 magnetometer. Diamagnetic corrections were made with Pascal's constants for all of the constituent atoms.

X-ray Measurements: Diffraction intensity data for single crystals of **1** and **2** were collected with a Rigaku Saturn CCD area detector diffractometer by employing graphite-monochromated Mo-K_α radiation (λ = 0.71073 Å). The structures were solved by direct methods and refined by full-matrix least-squares on F^2 by using SHELXS 97[40] and SHELXL 97[41] programs, respectively. Non-hydrogen atoms were refined anisotropically and hydrogen atoms were placed in calculated positions and refined isotropically by using a riding model. Pertinent crystallographic data and structure refinement parameters are summarized in Table 2. CCDC-759421 (for **1**) and -759422 (for **2**) contain the supplementary crystallographic data for this paper. These data can be obtained free of charge from The Cambridge Crystallographic Data Centre via www.ccdc.cam.ac.uk/data_request/cif.

Synthesis of Complex 1: To a MeOH solution (20 mL) of $Mn(ClO_4)_2\cdot6H_2O$ (74.2 mg, 0.2 mmol) was added $Na(HCOO)\cdot2H_2O$ (54.4 mg, 0.4 mmol) and H_2L (40.8 mg, 0.2 mmol) and then $NaOCH_3$ (43.2 mg, 0.8 mmol) was added. After stirring for 1 h, a dark-green solution was formed, which was allowed to slowly evaporate for one week, giving dark-green block crystals of **1**. The crystals were collected by filtration and washed with cold MeOH and Et_2O. Yield: 28.9 mg (42%). $C_{43}H_{70}Mn_3N_3O_{15}$ (1033.84): calcd. C 49.96, H 6.82, N 4.06; found C 49.25, H 6.45, N 3.97. IR (KBr): $\tilde{\nu}$ = 3449 (w), 1585 (m), 1427 (m), 1268 (m), 1122 (s), 1065 (s), 992 (m), 951 (m), 864 (m), 618 (m), 559 (m), 538 (m), 515 (m) cm^{-1}.

Synthesis of Complex 2: A mixture of $Mn(ClO_4)_2\cdot6H_2O$ (74.2 mg, 0.2 mmol), NaN_3 (52.0 mg, 0.8 mmol), and H_2L (40.8 mg, 0.2 mmol) in EtOH (20 mL) was stirring for 10 h, resulting in a color change to brown-green. Black block crystals suitable for X-ray crystallography formed after 7 days. The crystals were collected by filtration and washed with cold MeOH and Et_2O. Yield: 23.2 mg (35%). $C_{42}H_{65}Mn_3N_6O_{11}$ (994.81): calcd. C 50.71, H 6.59, N 8.45; found C 50.32, H 6.15, N 8.82. IR (KBr): $\tilde{\nu}$ = 3451 (w), 2092 (s), 1636 (m), 1540 (m), 1425 (m), 1286 (m), 1234 (m), 1208 (m), 1066 (m), 951 (m), 834 (m), 806 (m), 773 (m), 734 (m), 638 (m), 555 (m), 516 (m) cm^{-1}.

Acknowledgments

This work was supported by the National Science Foundation of China (Nos. 50672037, 20971072, 90922032) and the National Science Foundation of Tianjin (No. 09JCYBJC05600).

[1] D. Gatteschi, R. Sessoli, *Angew. Chem. Int. Ed.* **2003**, *42*, 268–297.
[2] a) M. N. Leuenberger, D. Loss, *Nature* **2001**, *410*, 789–793; b) S. Hill, R. S. Edwards, N. Aliaga-Alcalde, G. Christou, *Science* **2003**, *302*,1015–1018.
[3] a) R. Sessoli, H.-L. Tsai, A. R. Schake, S. Wang, J. B. Vincent, K. Folting, D. Gatteschi, G. Christou, D. N. Hendrickson, *J. Am. Chem. Soc.* **1993**, *115*, 1804–1816; b) G. Christou, D. Gatteschi, D. N. Hendrickson, R. Sessoli, *MRS Bull.* **2000**, *25*, 66–71.
[4] L. Bogani, A. Vindigni, R. Sessoli, D. Gatteschi, *J. Mater. Chem.* **2008**, *18*, 4750–4758.
[5] E. Coronado, P. Day, *Chem. Rev.* **2004**, *104*, 5419–5448.
[6] R. Sessoli, D. Gatteschi, A. Caneschi, M. A. Novak, *Nature* **1993**, *365*, 141–143.
[7] D. Gatteschi, A. L. Barra, A. Caneschi, A. Cornia, R. Sessoli, L. Sorace, *Coord. Chem. Rev.* **2006**, *250*, 1514–1529.
[8] G. Rogez, B. Donnio, E. Terazzi, J. L. Gallani, J. P. Kappler, J. P. Bucher, M. Drillon, *Adv. Mater.* **2009**, *21*, 4323–4333.

[9] G. Redler, C. Lampropoulos, S. Datta, C. Koo, T. C. Stamatatos, N. E. Chakov, G. Christou, S. Hill1, *Phys. Rev. B* **2009**, *80*, 094408.
[10] M. Atanasov, P. Comba, S. Hausberg, B. Martin, *Coord. Chem. Rev.* **2009**, *253*, 2306–2314.
[11] D. Gatteschi, R. Sessoli, J. Villain, *Molecular Nanomagnets*, Oxford University Press, New York, **2006**.
[12] a) S. Osa, T. Kido, N. Matsumoto, N. Re, A. Pochaba, J. Mroziński, *J. Am. Chem. Soc.* **2004**, *126*, 420–421; b) C. M. Zaleski, E. C. Depperman, J. W. Kampf, M. L. Kirk, V. L. Pecoraro, *Angew. Chem. Int. Ed.* **2004**, *43*, 3912–3914; c) H. Oshio, M. Nihei, S. Koizumi, T. Shiga, H. Nojiri, M. Nakano, N. Shirakawa, M. Akatsu, *J. Am. Chem. Soc.* **2005**, *127*, 4568–4569; d) J.-P. Costes, F. Dahan, W. Wernsdorfer, *Inorg. Chem.* **2006**, *45*, 5–7.
[13] A. J. Tasiopoulos, W. Wernsdorfer, B. Moulton, M. J. Zaworotko, G. Christou, *J. Am. Chem. Soc.* **2003**, *125*, 15274–15275.
[14] a) A. Mishra, W. Wernsdorfer, S. Parsons, G. Christou, E. K. Brechin, *Chem. Commun.* **2005**, 2086–2088; b) M. Murugesu, A. Mishra, W. Wernsdorfer, K. A. Abboud, G. Christou, *Polyhedron* **2006**, *25*, 613–625.
[15] H. Miyasaka, M. Julve, M. Yamashita, R. Clérac, *Inorg. Chem.* **2009**, *48*, 3420–3437.
[16] A. Caneschi, D. Gatteschi, N. Lalioti, C. Sangregorio, R. Sessoli, G. Venturi, A. Vindigni, A. Rettori, M. G. Pini, M. A. Novak, *Angew. Chem. Int. Ed.* **2001**, *40*, 1760–1763.
[17] H. Miyasaka, M. Yamashita, *Dalton Trans.* **2007**, 399–406.
[18] H. Miyasaka, T. Madanbashi, K. Sugimoto, Y. Nakazawa, W. Wernsdorfer, K.-i. Sugiura, M. Yamashita, C. Coulon, R. Clérac, *Chem. Eur. J.* **2006**, *12*, 7028–7040.
[19] a) R. Clérac, H. Miyasaka, M. Yamashita, C. Coulon, *J. Am. Chem. Soc.* **2002**, *124*, 12837–12844; b) E. Pardo, R. Ruiz-García, F. Lloret, J. Faus, M. Julve, C. Ruiz-Pérez, *Adv. Mater.* **2004**, *16*, 1597–1600; c) E. Pardo, R. Ruiz-García, F. Lloret, J. Faus, M. Julve, Y. Journaux, M. A. Novak, F. S. Delgado, C. Ruiz-Pérez, *Chem. Eur. J.* **2007**, *13*, 2054–2066; d) M. Ferbinteanu, H. Miyasaka, W. Wernsdorfer, K. Nakata, K. Sugiura, M. Yamashita, C. Coulon, R. Clérac, *J. Am. Chem. Soc.* **2005**, *127*, 3090–3099; e) R. Lescouëzec, J. Vaissermann, C. Ruiz-Pérez, F. Lloret, R. Carrasco, M. Julve, M. Verdaguer, Y. Dromzée, D. Gatteschi, W. Wernsdorfer, *Angew. Chem. Int. Ed.* **2003**, *42*, 1483–1486; f) L. M. Toma, R. Lescouëzec, J. Pasán, C. Ruiz-Pérez, J. Vaissermann, J. Cano, R. Carrasco, W. Wernsdorfer, F. Lloret, M. Julve, *J. Am. Chem. Soc.* **2006**, *128*, 4842–4853.
[20] S. W. Choi, H. Y. Kwak, J. H. Yoon, H. C. Kim, E. K. Koh, C. S. Hong, *Inorg. Chem.* **2008**, *47*, 10214–10216.
[21] J.-P. Costes, J. M. Clemente-Juan, F. Dahan, J. Milon, *Inorg. Chem.* **2004**, *43*, 8200–8202.
[22] a) L. Bogani, C. Sangregorio, R. Sessoli, D. Gatteschi, *Angew. Chem. Int. Ed.* **2005**, *44*, 5817–5821; b) K. Bernot, L. Bogani, A. Caneschi, D. Gatteschi, R. Sessoli, *J. Am. Chem. Soc.* **2006**, *128*, 7947–7956.
[23] T.-F. Liu, D. Fu, S. Gao, Y.-Z. Zhang, H.-L. Sun, G. Su, Y.-J. Liu, *J. Am. Chem. Soc.* **2003**, *125*, 13976–13977.
[24] a) K. Bernot, J. Luzon, R. Sessoli, A. Vindigni, J. Thion, S. Richeter, D. Leclercq, J. Larionova, A. v. d. Lee, *J. Am. Chem. Soc.* **2008**, *130*, 1619–1627; b) H.-B. Xu, B.-W. Wang, F. Pan, Z.-M. Wang, S. Gao, *Angew. Chem. Int. Ed.* **2007**, *46*, 7388–7392; c) C.-M. Liu, D.-Q. Zhang, D.-B. Zhu, *Inorg. Chem.* **2009**, *48*, 4980–4987; d) J. H. Yoon, D. W. Ryu, H. C. Kim, S. W. Yoon, B. J. Suh, C. S. Hong, *Chem. Eur. J.* **2009**, *15*, 3661–3665; e) S. W. Przybylak, F. Tuna, S. J. Teat, R. E. P. Winpenny, *Chem. Commun.* **2008**, 1983–1985.
[25] Y.-Z. Zheng, Y.-h. Lan, W. Wernsdorfer, C. E. Anson, A. K. Powell, *Chem. Eur. J.* **2009**, *15*, 12566–12570.
[26] Z.-M. Sun, A. V. Prosvirin, H.-H. Zhao, J.-G. Mao, K. R. Dunbar, *J. Appl. Phys.* **2005**, *97*, 10B305.
[27] a) X.-T. Liu, X.-Y. Wang, W.-X. Zhang, P. Cui, S. Gao, *Adv. Mater.* **2006**, *18*, 2852–2856; b) Y.-L. Bai, J. Tao, W. Wernsdorfer, O. Sato, R.-B. Huang, L.-S. Zheng, *J. Am. Chem. Soc.* **2006**, *128*, 16428–16429.
[28] a) J. Tao, Y.-Z. Zhang, Y.-L. Bai, O. Sato, *Inorg. Chem.* **2006**, *45*, 4877–4879; b) C.-M. Liu, D.-Q. Zhang, D.-B. Zhu, *Chem. Commun.* **2008**, 368–370; c) J. Kim, J. M. Lim, Y. Do, *Eur. J. Inorg. Chem.* **2003**, 2563–2566; d) M. Viciano-Chumillas, S. Tanase, I. Mutikainen, U. Turpeinen, L. J. de Jongh, J. Reedijk, *Inorg. Chem.* **2008**, *47*, 5919–5929.
[29] M. Viciano-Chumillas, S. Tanase, I. Mutikainen, U. Turpeinen, L. J. de Jongh, J. Reedijk, *Dalton Trans.* **2009**, 7445–7453.
[30] V. H. Crawford, H. W. Richardson, J. R. Wasson, D. J. Hodgson, W. E. Hatfield, *Inorg. Chem.* **1976**, *15*, 2107–2110.
[31] Y.-Z. Zheng, M.-L. Tong, W.-X. Zhang, X.-M. Chen, *Angew. Chem. Int. Ed.* **2006**, *45*, 6310–6314.
[32] N. Ishii, Y. Okamura, S. Chiba, T. Nogami, T. Ishida, *J. Am. Chem. Soc.* **2008**, *130*, 24–25.
[33] D. Gatteschi, R. Sessoli, J. Villain, *Molecular Nanomagnets*, Oxford University Press, New York, **2006**, pp. 69–75.
[34] W. Hibbs, D. K. Rittenberg, K.-i. Sugiura, B. M. Burkhart, B. G. Morin, A. M. Arif, L. Liable-Sands, A. L. Rheingold, M. Sundaralingam, A. J. Epstein, J. S. Miller, *Inorg. Chem.* **2001**, *40*, 1915–1925.
[35] J. A. Mydosh, *Spin Glasses*, *An Experimental Introduction*, Taylor and Francis, London, **1993**.
[36] Y.-Z. Zheng, W.-Xue, W.-X. Zhang, M.-L. Tong, X.-M. Chen, F. Grandjean, G. J. Long, S. W. Ng, P. Panissod, M. Drillon, *Inorg. Chem.* **2009**, *48*, 2028–2042.
[37] C. Coulon, R. Clérac, L. Lecren, W. Wernsdorfer, H. Miyasaka, *Phys. Rev. B* **2004**, *69*, 132408.
[38] T. V. Hansen, L. Skattebol, *Tetrahedron Lett.* **2005**, *46*, 3829–3830.
[39] F. Qiu, L.-C. Wang, Y. Dong, *Zhongguo Yaowu Huaxue Zazhi* **2003**, *13*, 353–355.
[40] G. M. Sheldrick, *SHELXS 97, Program for Crystal Structure Solution*, University of Göttingen, **1997**.
[41] G. M. Sheldrick, *SHELXL 97, Program for Crystal Structure Refinement*, University of Göttingen, **1997**.

Received: December 24, 2009
Published Online: March 9, 2010

